The Simulations and Comparison of Visibility Measurements by Digital Image Processing

Meng-Sain Huang, Dai-Ling Tsai, Jiun-Jian Liaw*

Department of Information and Communication Engineering,

Chaoyang University of Technology

{s10030612, s9830625, jjliaw}@cyut.edu.tw

168 Jifong E. Rd., Wufong District, Taichung, Taiwan (R.O.C)

***Abstract*—The measurement of visibility has been made in digital image processing when technologies development currently, for example, more and more works are done with machinery or instruments substituting for manpower. Considering existing nonstandard image processing methods, we propose an experimental method including four manners such as ideal high-pass filter, homomorphic filter, intensified Haar function and gray scale contrast for measurement of visibility. In this research, the accurate visibility index based on experiments with smog affecting visibility of an image is determined by referring to the relationship between illumination and the visibility index.**

Keywords—Visibility estimate, Digital image processing, Filter

1. INTRODUCTION

Visibility is an indicator to present atmospheric turbidity wherein prevailing visibility is defined as the horizontal distance of the farthest dark object in different directions recognized by a trained observer in a high place [1]. The measurement of visibility is made through visual inspection or instruments, for example, expensive laser tester and digital processing discussed in this research [2].

The digital image processing which facilitates our works has evolved lots of practical applications such as meteorological observation [3], security management [4], face recognition [5] and license plate recognition [6]. In this regard, the measurement of visibility is one topic among various applications in meteorological observation [7]. In literatures published in the past, Bayot et al. determined multiple visibility indices by analyzing contrasts and HSVs of images [8]; Martha et al. analyzed contrasts and gray scales of images to acquire the visibility index based on different weights [9]; Yuan et al. effectuated an automated visibility observation system by analyzing gray scales and deciding the visibility index [10]; Hautiere et al. built a roadway visibility monitoring system for traffic control based on estimated visibility [11].

One method of measuring visibility of an image refers to the image's gray scale [10]. As two parts of one image, sky (background) and buildings (objects), for example, which cannot be identified in a low-visibility environment (or clearly recognized in a high-visibility environment), denote their approximate (or contrasted) gray scales. According to this principle, a visibility index value can be determined.

An alternative method of measuring visibility of an image is based on the image's contrast [8][9]. The contrast of one image checked in a good (bad) visibility environment is relatively high (or low). Moreover, the relationship between contrast and visibility can be taken as an indicator to measure visibility.

The visual inspection as the basis for measurement of visibility of digital images mostly [12] is not as accurate as instruments because of personal errors. Accordingly, an experimental method is presented in this research as the standard to measure visibility.

2. VISIBILITY INDEX VALUE

In this research, we introduce methods for measurement of visibility including ideal high-pass filter, homomorphic filter, intensified Haar function and gray scale contrast, all of which are compared in experiments.

2.1. Ideal High-pass Filter

According to the Fourier transform, a digital image with a size of $M*N$ is indicated as follows:

$$FI(u,v)=\frac{1}{MN}\sum_{x=0}^{M-1}\sum_{y=0}^{N-1}I(x,y)\exp\left[-j2\pi\left(\frac{ux}{M}+\frac{vy}{N}\right)\right] \quad (1)$$

where $I(x,y)$ means the pixel at a coordinate (x,y) in an image. In Equation (1), the frequencies less than (or greater than) D_0 as a threshold frequency should be filtered (or preserved) by the ideal high-pass filter, as shown in Equation (2).

$$HP(u,v)=\begin{cases}0 & \text{if } D(u,v)\le D_0\\ 1 & \text{if } D(u,v)> D_0\end{cases} \quad (2)$$

where D_0 is a positive integral and $D(u,v)$ is a distance from a coordinate (u,v) to an image's center. Then, the filtered images are derived from results in Equation (1) through the inverse Fourier transform. Finally, the visibility index is determined with the average of gray scale values calculated.

2.2. Homomorphic Filtering

Uneven brightness attributed to light-induced shadows is usually observed in an image with its visibility to be measured. In this regard, the local contrast of the image should be intensified for presenting more information related to darker objects in the image. In one image consisting of bright and dark pixels, the brightness of any object in the image is presented by light projected on the object and reflected light from the object. As brightness of a pixel at a coordinate (x,y) in an image, $I(x,y)$ is a product of illumination and reflectance as shown in Equation (3).

$$I(u,v)=i(x,y)r(x,y) \quad (3)$$

where $i(x,y)$ is illumination and $r(x,y)$ is reflectance. With the Fourier transform conducted, the illumination components and the reflectance components are classified as low-frequency parts and high-frequency parts, respectively. Based on adjustable components such as $i(x,y)$ and $r(x,y)$, the above method is in favor of intensifying or attenuating information in an image.

The transition function $H(u,v)$ of a homomorphic filter which is the filter depending on regulating illumination and reflectance components for ideal control is defined in Equation (4).

$$H(u,v)=(H-L)\left[1-\exp\left(-\frac{D^2(u,v)}{D_0}\right)\right]+L \quad (4)$$

where L and H are parameters presenting low-frequency and high-frequency information to be intensified or attenuated, respectively. In the case of $L<1$ and $H>1$, illumination descends but reflectance ascends. In this research, we assume $L=0.5$ and $H=1.1$. The high-frequency information which passes a homomorphic filter is further retrieved by a two-dimensional Gaussian high-pass filter which is defined in Equation (5).

$$G(u,v)=1-\exp\left(-\frac{D^2(u,v)}{D_0}\right) \quad (5)$$

The visibility index is determined with the average of gray scale values calculated.

2.3. Sharpness with Haar Function

The Haar function presents the orthogonal base of a wavelet transform and the number of Haar filters is $1/\sqrt{2}$. Therefore, both inputs, I_1 and I_2, are divided into two frequency bands, $(I_1-I_2)/\sqrt{2}$ and $(I_1+I_2)/\sqrt{2}$.

For inputs $I(x,y)$ ($0\le x\le M-1$ and $0\le y\le N-1$) of one image, the values on x and y directions to be calculated are indicated in Equations (6) and (7).

$$I_1=I(2m,y) \quad (6)$$

$$I_2=I(2m+1,y) \quad (7)$$

I_1 and I_2 are inputs for the Haar function ($0\le m\le M/2$). In addition, the translations of pixels are presented in the inputs to be transformed, e.g., I_1 and I_2 in Equations (8) and (9).

$$I_1=I(2m+1,y) \quad (8)$$

$$I_2=I(2m+2,y) \quad (9)$$

Similarly, the translation of a pixel is also presented in each of two inputs on the y direction to be transformed. The first group of inputs on the y direction is indicated in Equations (10) and (11).

$$I_1=I(x,2n) \quad (10)$$

$$I_2=I(x,2n+1) \quad (11)$$

The second group of inputs is indicated in Equations (12) and (13).

$$I_1=I(x,2n+2) \quad (12)$$

$$I_2=I(x,2n+2) \quad (13)$$

Where $0\le n\le N/2$. In other words, four sub-images are derived from the initial information through the Haar transform.

Then, the initial data (I_1 and I_2) is transformed to the intensified data (I_1' and I_2') based on positive or negative information $(I_1-I_2)/\sqrt{2}$. For positive $(I_1-I_2)/\sqrt{2}$, Equations (14) and (15) are applicable.

$$I_1' = 14\log(I_1 - I_2 + 1) \quad (14)$$

$$I_2' = 0 \quad (15)$$

Otherwise, Equations (16) and (17) are applicable for negative information $(f_1 - f_2)/\sqrt{2}$.

$$I_1' = 0 \quad (16)$$

$$I_2' = 14\log(I_1 - I_2 + 1) \quad (17)$$

Finally, the intensified image is developed with four intensified sub-images added.

2.4. Gray Scale Contrast

The method to determine visibility of one image proposed by Martha et al. is based on parameters of an image such as gray scale and contrast. In this regard, the gray scale of one image is first determined by Weber contrast, as shown in Equation (18).

$$W = \frac{Io - Ib}{Ib} \quad (18)$$

where *W*, *Io* and *Ib* are the gray scale of one image, the average brightness of objects, and the average brightness of background, respectively.

On the other hand, the contrast should be decided for the dynamic ranges of an image, i.e., local dynamic range and global dynamic range.

The visibility index value is derived from three parameters coordinating their distinct weights, as shown in Equation (19).

$$GC = GD*0.3 + LD*0.35 + W*0.35 \quad (19)$$

where *DG* and *DL* mean the global dynamic range and the local dynamic range, respectively. The visibility index value, *GC*, is determined with *DG*, *DL* and *W* multiplied by three distinct weights whose sum is equal to 1.

As shown in Equation (20), the optimal weights for three parameters derived in our experiments differ from those of other literatures in which different objects were measured.

$$GC = GD*0.6 + LD*0.3 + W*0.1 \quad (20)$$

3. Experimental Method

In this research, the experimental method is distinct from those of other literatures for measurement of an image's visibility, most of which relied on comparisons of visual inspections with personal errors.

As shown in Fig. 1, the experiments are conducted in a transparent glass box with one image fixed on one end, a camera installed on the opposite end for capturing the image, and an illuminometer underneath to measure illumination and brightness. The experiments to be recorded in a video tape start with smog fed into the box.

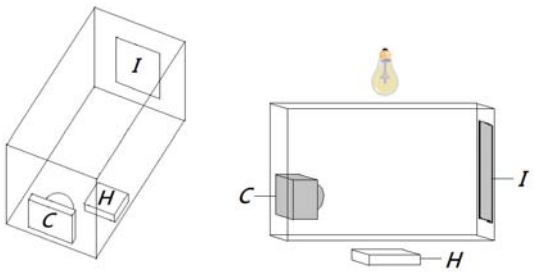

(a) (b)

Fig. 1 Environment of Experiment 1:
(a) top view; (b) side view
(I: image, H:lux meter, C: camera)

In this research, the camera model is SONY W55 with the image resolution of 640*480. In Experiment 1 under recording, darkened illumination from 1250lux to 930lux and worse visibility emerge gradually with smog fed into the box. The visibility for recorded images is measured according to four methods presented herein. Fig. 6 illustrates an image for measurement of visibility.

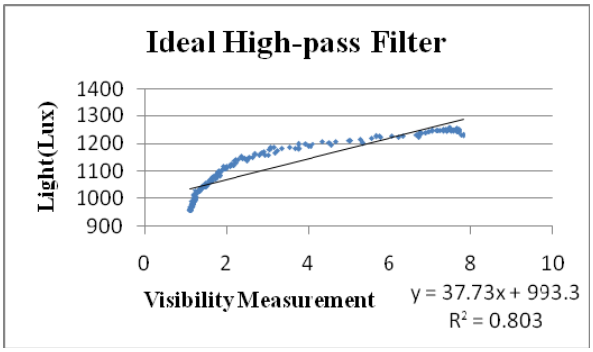

Fig. 2 Visibility Measurement of Ideal High-pass Filter in Experiment 1

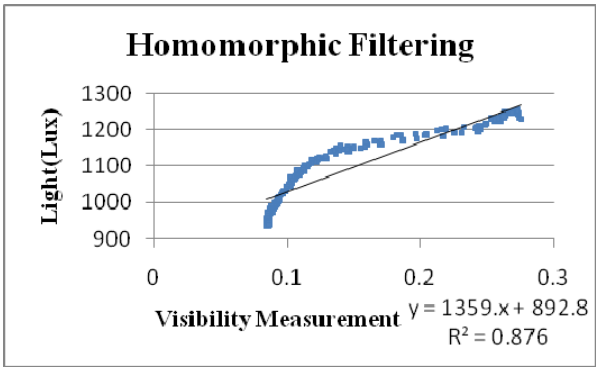

Fig. 3 Visibility Measurement of Homomorphic Filtering in Experiment 1

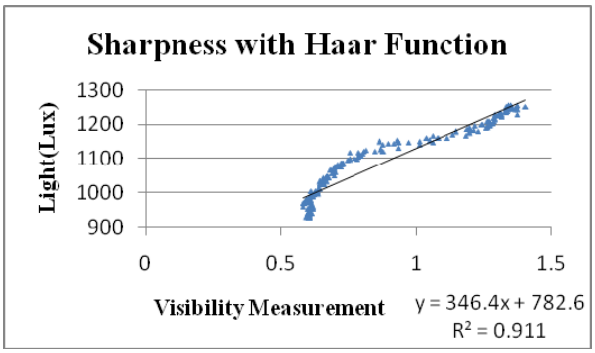

Fig. 4 Visibility Measurement of Sharpness with Haar Function in Experiment 1

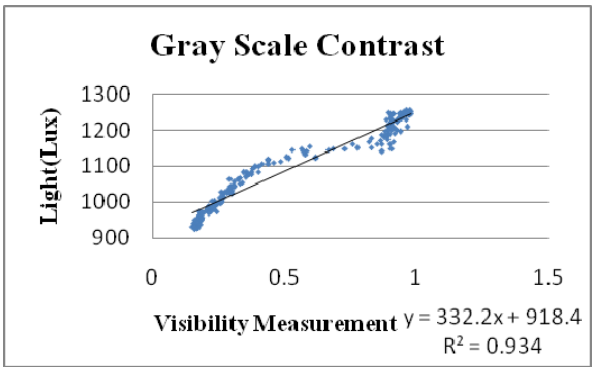

Fig. 5 Visibility Measurement of Gray Scale Contrastin Experiment 1

Fig. 6 Source image of Experiment 1

In Experiment 2, another object is added into the scene, for example, a skyscraper model between the original image and the camera, by which an image presenting depth-of-field is captured. As shown in Fig. 7, the skyscraper model is parallel to and separated from the image by 5cm. The video tape is also recorded as is the video tape in Experiment 1 for measurement of visibility based on four methods presented herein. Fig. 12 illustrates an image for measurement of visibility.

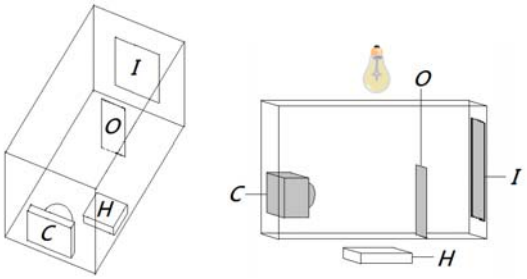

(a) (b)

Fig. 7 Environment of Experiment 2: (a) top view; (b) side view (I: image, H:lux meter, C: camera, O: objective)

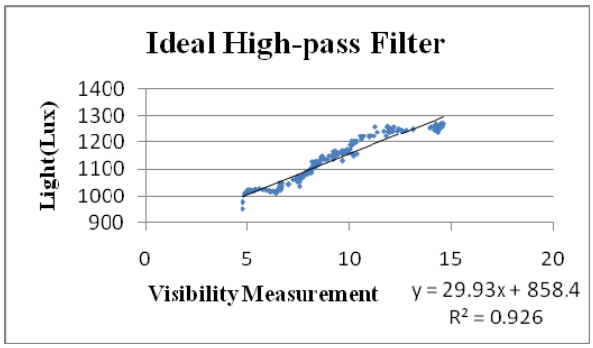

Fig. 8 Visibility Measurement of Ideal High-pass Filter in Experiment 2

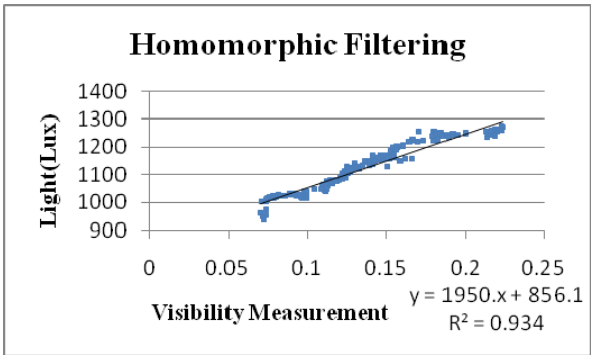

Fig. 9 Visibility Measurement of Homomorphic Filtering in Experiment 2

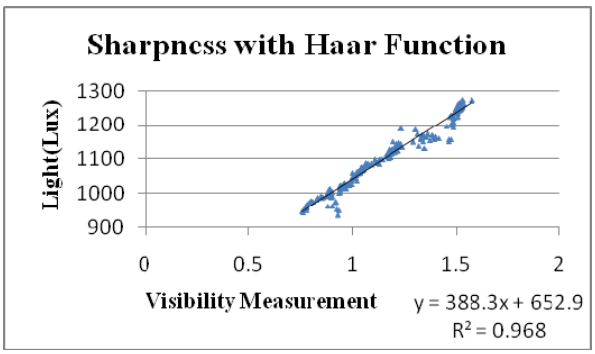

Fig. 10 Visibility Measurement of Sharpness with Haar Function in Experiment 2

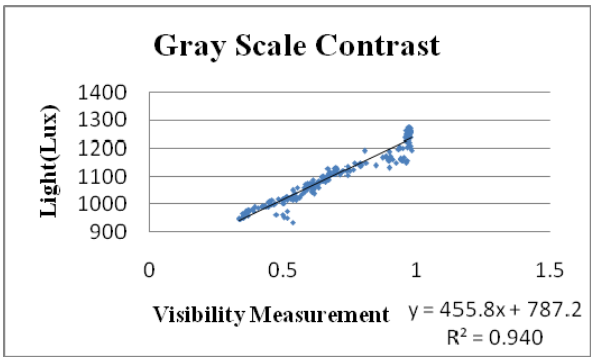

Fig. 11 Visibility Measurement of Gray Scale Contrast in Experiment 2


Fig. 12 Source image of Experiment 2

4. CONCLUSION

From Experiment 1 that the R^2 values with weights modified in two methods, gray scale contrast and intensified Haar function, are 0.934 and 0.911, respectively. In contrast, the R^2 value based on the ideal high-pass filter or the homomorphic filter is less than 0.9. In Experiment 2, the R^2 values based on four methods, i.e., intensified Haar function, gray scale contrast, homomorphic filter, and ideal high-pass filter, are 0.968, 0.94, 0.934 and 0.926, respectively.

The method of the intensified Haar function with the Fourier transform and the wavelet transform integrated proposed herein provides the more accurate visibility index value, particularly the visibility index value of an image presenting significant depth-of-field, than other methods for measurement of visibility without satisfactory accuracy.

REFERENCES

[1] 交通部中央氣象局，地面氣象測報作業規範，中央氣象局, 2004。

[2] Emmanuel P. Baltsavias, "A comparison between photogrammetry and laser scanning," ISPRS Journal of Photogrammetry and Remote Sensing, Volume 54, Issues 2–3, July 1999, Pages 83–94

[3] Xiaoying Cong, Balss U., Eineder M., Fritz T., "Imaging Geodesy—Centimeter-Level Ranging Accuracy With TerraSAR-X: An Update," IEEE Geoscience and Remote Sensing Letters, vol.9, no.5, pp.948-952, Sept. 2012

[4] Hassan H., Bakar R.A., Mokhtar A.T.F., "Face recognition based on auto-switching magnetic door lock system using microcontroller," 2012 International Conference on System Engineering and Technology (ICSET), pp.1-6, 11-12 Sept. 2012

[5] Jiwen Lu, Xiuzhuang Zhou, Yap-Peng Tan, Yuanyuan Shang, Jie Zhou, "Cost-Sensitive Semi-Supervised Discriminant Analysis for Face Recognition," IEEE Transactions on Information Forensics and Security, vol.7, no.3, pp.944-953, June 2012

[6] Swetha V., Sandeep D.R., "Automatic authorized vehicle recognition system," International Conference on Sustainable Energy and Intelligent Systems (SEISCON 2011), pp.789-790, 20-22 July 2011

[7] J.-J. Liaw, S.-B. Lian, Y.-F. Huang, and R.-C. Chen, “Using sharpness image with Haar function for urban atmospheric visibility measurement,” Aerosol and Air Quality Research, Vol. 10, No. 4, pp. 323-330, 2010.

[8] Bayot R.K.O., Labuguen R.T., Volante E.J.P., Libatique N.J.C., Tangonan G.L., "Urban visibility measurements during tropical weather events using image processing," TENCON 2012 - 2012 IEEE Region 10 Conference, pp.1,6, 19-22 Nov. 2012

[9] Guzman M., Restrepo A., “The image quality in the measurement of atmospheric visibility from contrast indices and edges,” Image, Signal Processing, and Artificial Vision (STSIVA), 2012 XVII Symposium of, pp.196-201, 12-14 Sept. 2012, Medellín, Colombia

[10] Chung-Shin Yuan, Cho-Ching Lo, Wei-Chin Chen, Chan-Chorn Chen, “Forecasting Atmospheric Visibility of Metropolitan Area Using an Automated Observation System,” For the presentation at the Air and Waste Management Association’s 97th Annual Meeting and Exhibition, June 22-25, Indianapolis, Indiana, USA

[11] Hautiere N., Boubezoul A., "Combination of Roadside and In-vehicle Sensors for Extensive Visibility Range Monitoring," Advanced Video and Signal Based Surveillance, 2009. AVSS '09. Sixth IEEE International Conference on , pp.388,393, 2-4 Sept. 2009

[12] C.-H. Luo, C.-Y. Wen, C.-S. Yuan, J.-J. Liaw, C.-C. Lo, and S.-H. Chiu, “Investigation of urban atmospheric visibility by high-frequency extraction: model development and field test,” Atmospheric Environment, Vol. 39, No. 14, pp. 2545-2552, 2005.